Andreas Prescher, M.D., Dominik Brors, M.D., and
Klaus von Ammon, M.D.

New Anatomical Description of the Cavernous Sinus Surface and Its Significance in Microsurgery

ABSTRACT—The anatomical and surgical approach to the sella region is of special interest for microsurgeons involved in ear, nose, and throat surgery, neurosurgery, ophthalmology, maxillofacial surgery, and skull base surgery. We investigated the surface morphology of the cavernous sinus and the sella turcica in 48 adult and 2 neonate specimens. To simplify the morphometric recording, distances between anatomical landmarks were defined. In addition, three triangles—the preinfundibular, the parasellar, and the internal carotid artery triangle—are introduced. These triangles are defined in order to determine the location where cranial nerves III, IV, V, and VI penetrate the dura with respect to the anterior and posterior clinoid processes and the tuberculum and dorsum sellae. The triangles were found to be symmetrical, with identical bilateral measurements, and the entry points of the cranial nerves were found to be constant. In 17 cases (34%), we found a dehiscence of the sellar diaphragm, and in 15 cases (30%), rope-like adhesions at the pituitary stalk.

The cavernous sinus and the sella turcica are important regions for microsurgeons treating carotid artery aneurysms; carotid-cavernous fistulae; cavernous sinus thrombosis; pituitary, orbital, and osseous tumors; and skull base inflammations. Cranial nerves III, IV, V, and VI and the internal carotid artery and its branches pass here through a very limited space. Therefore, precise orientation with respect to constant anatomical landmarks, including the surface morphology, is necessary for microsurgical and neuroendoscopic approaches with a limited field of vision, or "key-hole-surgery."[1]

Detailed descriptions of the architecture of the cavernous sinus are common in the anatomical literature,[2–14] whereas the surface structure is presented only cursorily. This study presents a precise description of the dorsal tip of the cavernous sinus and defines the entrance points of the cranial nerves by using simple geometric figures such as triangles, as proposed by Dolenc[15] and Umansky et al,[16] in relation to bony structures.

The transversal plate[14,17] of the cavernous sinus changes in medial direction toward the sella turcica, which is closed cranially by the sellar diaphragm. We investigated this region with regard to common variations such as dehiscences and rope-like adhesions.

MATERIALS AND METHODS

Specimens

The 48 specimens from adults (31 to 93 years old, 24 females and 24 males) were fixed in 4% buffered formaldehyde solution and used for the investigation.

We defined several distances and triangles involving anatomical structures that could be easily deter-

Skull Base Surgery, Volume 7, Number 4, 1997 Department of Anatomy, University Medical School of the RWTH, Aachen, Germany (A.P., D.B.) Department of Neurosurgery, University Hospital, Zürich, Switzerland (K.v.A.). Reprint requests: Dr. A. Prescher, Institut für Anatomie, Universitätsklinikum der RWTH Aachen, D-52057 Aachen, Germany.

mined by use of a caliper. The measurements were taken twice by two independent investigators at different times, and the two measurements for each distance were averaged.

For the investigation of meningeal variations, we used two additional specimens from male neonates. Figure 1 illustrates the details of anatomical measurements for microsurgery.

Definitions

Distances

1. Width of the dorsum sellae: Distance between the tips of the posterior clinoid processes (PCLPs)
2. Width of the sellar diaphragm: Distance between its most lateral points
3. Distance between the dural entrance of the oculomotor nerve and the anterior clinoid process (ACLP)
4. Distance between the dural entrance of the oculomotor nerve and the PCLP
5. Distance between the dural entrance of the trochlear nerve and the PCLP
6. Distance between the dural entrance of the trochlear nerve and the pore of the oculomotor nerve
7. Distance between the dural entrance of the trigeminal nerve and the pore of the trochlear nerve
8. Distance between the pores of the abducent and trigeminal nerves
9. Distance between the pore of the abducent nerve and the cranial point of the dorsum sellae in the midsaggital plane
10. Length of the posterior pretroclinoid fold, from the ventromedial tentorial edge to the PCLP
11. Length of the anterior petroclinoid fold, from the ventromedial tentorial edge to the ACLP

Triangles

We defined three triangles and measured the lengths of their sides. The edges of the triangles are formed by constant anatomical landmarks. The dural entrance points of the pituitary stalk, the cranial nerves, and the trunk of the internal carotid artery are determined by the orientation of the triangles.

1. **Preinfundibular triangle (Fig. 2)**
   Right and left border: From the point where the pituitary stalk penetrates the dura to the medial entrances of the right and left optic nerves, respectively
   Anterior border: Connecting the medial points of each optic nerve before entering the optic canal

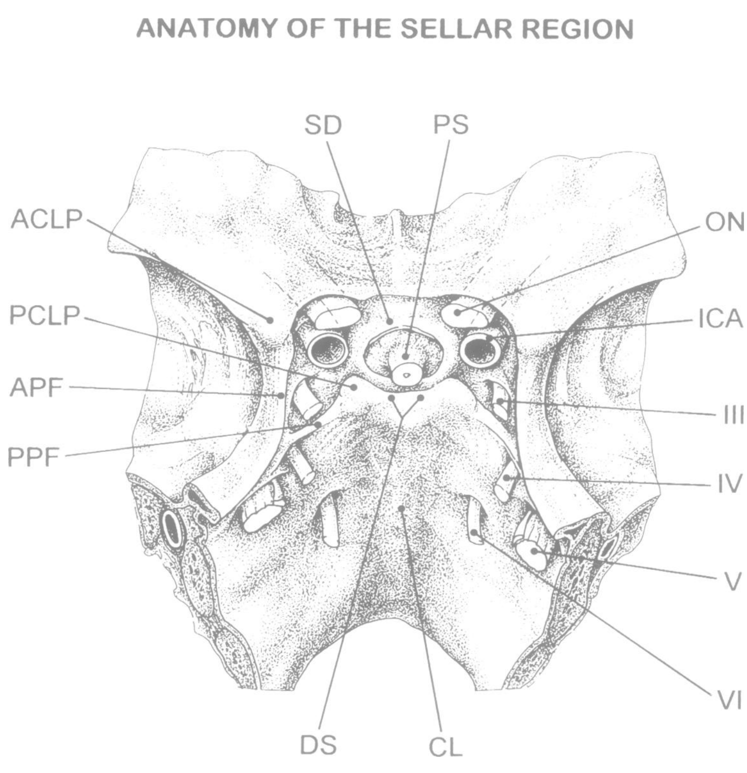

Figure 1. Schematic drawing of the normal anatomy of the sellar region. SD, sellar diaphragm; PS, pituitary stalk; ON, optic nerve; ICA, internal carotid artery; CL, clivus; DS, dorsum sellae; PPF, posterior petroclinoid fold; APF, anterior petroclinoid fold; PCLP, posterior clinoid process; ACLP, anterior clinoid process.

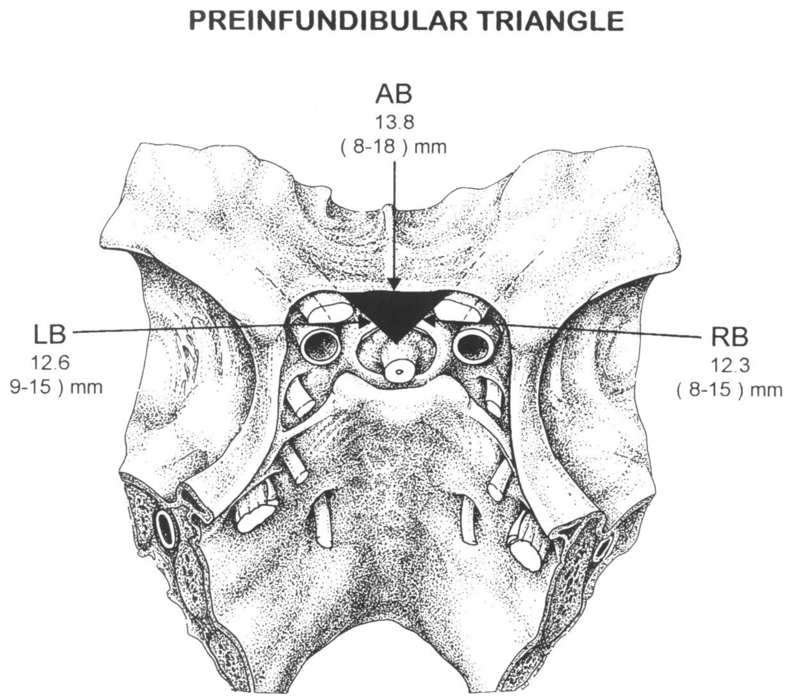

Figure 2. Schematic drawing of the preinfundibular triangle. LB, left border; RB, right border; AB, anterior border.

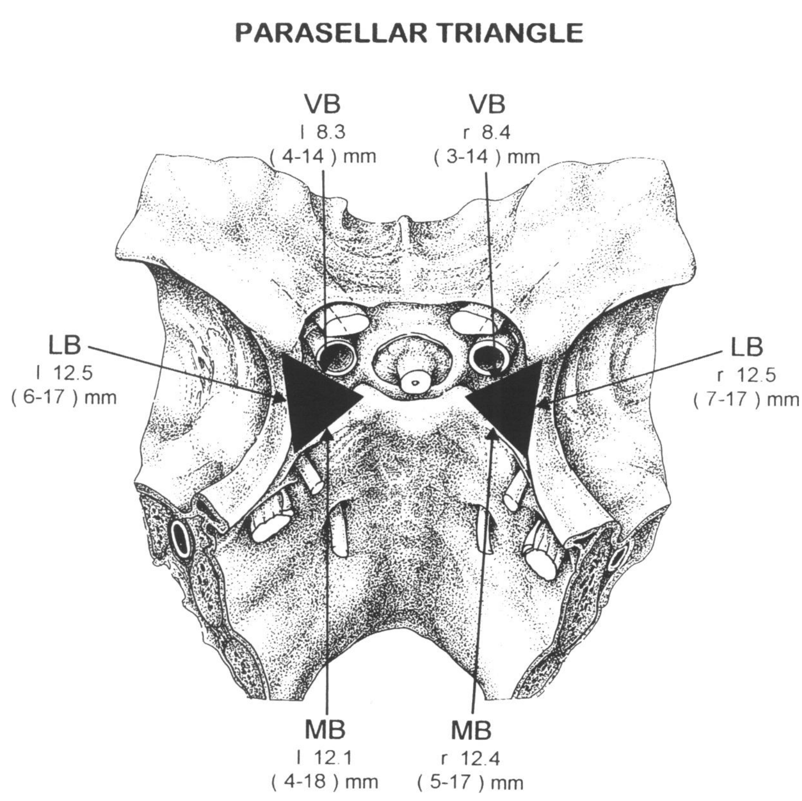

Figure 3. Schematic drawing of the parasellar triangle. LB, lateral border; VB, ventral border; MB, medial border.

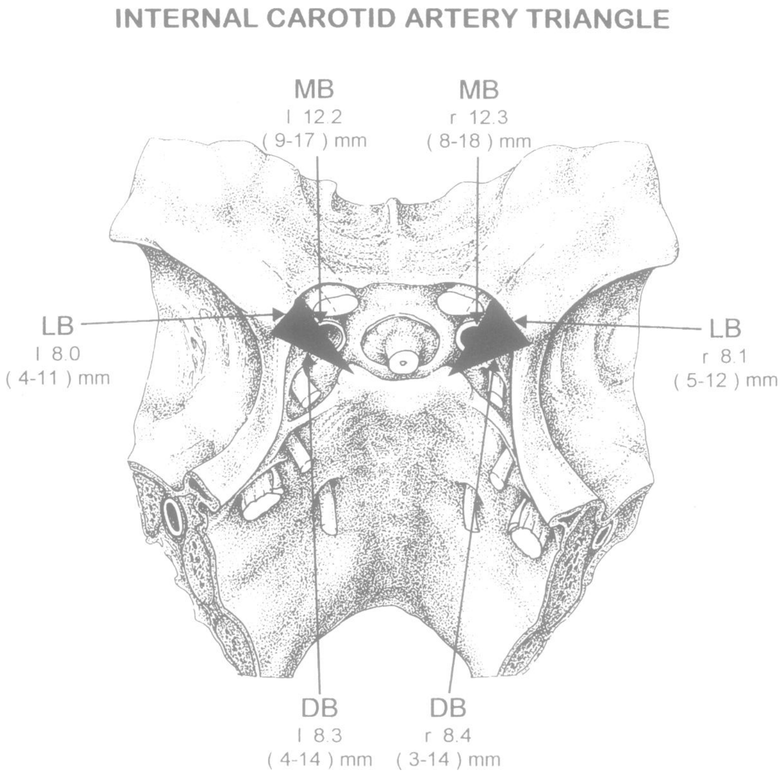

Figure 4. Schematic drawing of the internal carotid artery triangle. MB, medial border; LB, lateral border; DB, dorsal border.

2. **Parasellar triangle (Fig. 3)**
   Medial border: Length of the anterior petroclinoid fold, from the ventromedial tentorial edge to the ACLP
   Lateral border: Length of the posterior petroclinoid fold, from the ventromedial tentorial edge to the PCLP
   Ventral border: Connecting the ACLP to the PCLP
3. **Internal carotid artery triangle (Fig. 4)**
   Lateral border: Connecting the ACLP and the lateral point of the optic nerve just outside the optic canal
   Medial border: Connecting the PCLP and the lateral point of the optic nerve just outside the optic canal
   Posterior border: Connecting the ACLP to the PCLP

Variations in the Meningeal Morphology of the Sellar Region

We observed whether a dehiscence of the sellar diaphragm and rope-like adhesions around the pituitary stalk were present.

RESULTS

Distances

The measurements of the distances are given in Table 1.

Triangles

The measurements of the triangle sides are listed in Table 2. There are only minimal differences between the values for the left and right sides.

Variations of Meningeal Morphology of the Sellar Region

In 34% of the cases, a dehiscence of the sellar diaphragm (Fig. 5) was obvious. The dehiscence varied from 3 to 8 mm in diameter. In most cases (66%), the diaphragm surrounded the pituitary stalk like a collar (Fig. 6). Additionally, in 15 cases (30%), we found rope-like adhesions around the pituitary stalk (Fig. 7). Two specimens (4%) showed an accessory posterior petroclinoid fold (Fig. 8). In all cases, the anterior and the posterior petroclinoid folds determined a constant triangle configuration.

DISCUSSION

In modern microsurgery, orientation on landmarks of surface structures under normal and pathological conditions is absolutely necessary because of the limitations of the view field, especially in neuroendoscopy.[1]

Table 1. Distances Used for the Description of the Surface Morphology of the Sella Turcica

Stretch as Defined in Materials and Methods	*Average Distance (mm)*		*Range (mm)*	
	Left	*Right*	*Left*	*Right*
1. Width of dorsum sellae	15.5		8–22	
2. Width of sellar diaphragm	9.9		5–17	
3. Nerve (N.) III to ACLP	8.4	8.3	5–13	4–11
4. N. III to PCLP	5.5	5.5	3–10	2–11
5. N. IV to PCLP	12.6	12.7	6–18	9–15
6. N. III to N. IV	11.3	10.8	9–16	6–16
7. N. V to N. IV	5.1	5.2	2–11	3–10
8. N. V to N. VI	6.9	6.9	3–11	4–12
9. N. VI to middle of dorsum sellae	20.3	19.9	14–28	15–26
10. Length of posterior petroclinoid fold	12.1	12.4	4–18	5–17
11. Length of anterior petroclinoid fold	12.5	12.5	6–17	7–17

Distances were determined twofold independently. The numbers in the first column refer to the section on distances in Materials and Methods. Left and right refer to the left- and right-hand side of the skull, respectively.

Table 2. Measurements of the Triangles

	Average Distance (mm)		*Range (mm)*	
	Left	*Right*	*Left*	*Right*
1. Preinfundibular triangle (see Fig. 2)				
Right border	12.3		8–15	
Left border	12.6		9–15	
Anterior border	13.8		8–18	
2. Parasellar triangle (see Fig. 3)				
Medial border	12.1	12.4	4–18	5–17
Lateral border	12.5	12.5	6–17	7–17
Ventral border	8.3	8.4	4–14	3–14
3. Internal carotid artery triangle (see Fig. 4)				
Medial border	12.2	12.3	9–17	8–18
Lateral border	8.0	8.1	4–11	5–12
Dorsal border	8.3	8.4	4–14	3–14

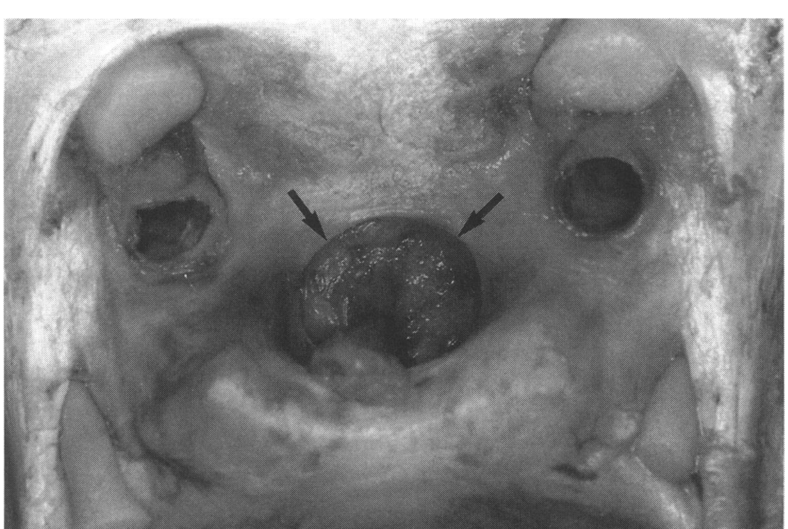

Figure 5. Large dehiscence of the sellar diaphragm in an 88-year-old woman. Note the sharp dural ridge (arrows) in the peripheral area of the sella.

Figure 6. Normal configuration with closed sellar diaphragm. The diaphragm surrounds the pituitary stalk like a collar.

Essential landmarks in the parasellar region are the ACLPs and PCLPs, tuberculum and dorsum sellae, pituitary stalk, and dural entrance points of cranial nerves III, IV, V, and VI. This normal surface morphology can be altered by, for example, aneurysms, tumors, or inflammations.[18,19]

The classic anatomical descriptions[2-14] give an excellent but so-called static overview of the structures. The microsurgical approach through the basal cisterns, on the other hand, is characterized by a dynamic, everchanging perspective in a limited field of view[19-21] (Fig. 9). It is oriented by the dural, sulcal, and arachnoid openings and guided by the sides and angles of defined triangles. Orientation on landmarks is mandatory during the procedures of cerebrospinal fluid release, sulcal and fissural opening, and tumor debulking because of the changing views of important and vital structures.[18,19] Therefore, it is essential to collect knowledge about as many anatomical landmarks, measurements, and interdependencies between these orientation points as possible. Such interdependencies can be easily described by the use of geometric figures such as triangles. Accordingly, we defined three triangles that should make the surgeons' work during various approaches easier: The preinfundibular triangle facilitates the frontal approach, the parasellar and internal carotid artery triangles facili-

Figure 7. Sellar diaphragm with fibrous strands (arrow) to the pituitary stalk in a 62-year-old woman.

Figure 8. Normal configuration of the sellar diaphragm, but accessory petroclinoid fold (arrow) caudally situated to the posterior petroclinoid fold. This specimen was taken from a 58-year-old man.

tate the frontotemporal orbitozygomatic (pterional) approach (Fig. 10), and the internal carotid artery triangle also helps in the subtemporal approach. Because these triangles are relatively constant and symmetrical, a deformation, even a slight one, can indicate a pathological lesion such as meningeoma, optic glioma, intraosseus or cavernous cranial nerve schwannoma, pituitary macroadenoma or carcinoma, chordoma, angiofibroma, vascular malformations (e.g., giant aneurysm of the internal carotid artery), intra- or suprasellar cysts (e.g., of Rathke's pouch, colloid, or arachnoid), bulging "empty sella" filled with cerebrospinal fluid, or inflammation involving the skull base and meninges (e.g., tuberculosis, sarcoidosis, and actinomycosis).

Preoperative diagnosis of the parasellar region depends on magnetic resonance imaging (MRI), computed tomography (CT scan), and angiography.[22,23] MRI is the preferred neuroimaging technique because it allows direct visualization of pathological lesions, deformation of adjacent structures, and normal anatomy of soft tissue.[24,25] Even with high-resolution imaging, some delicate surface structures (e.g., the sellar diaphragm and rope-like adhesions) are seldom visible and distinguishable from adjacent tissue. CT scan, especially in its

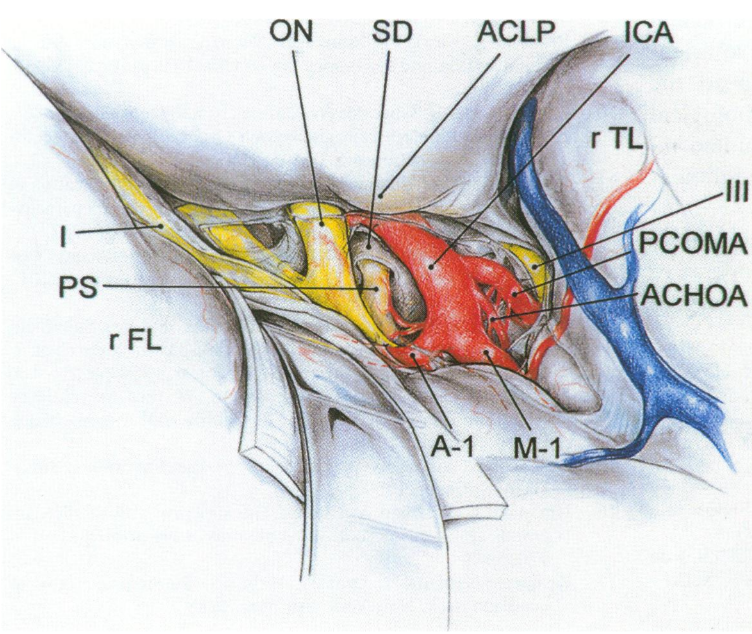

Figure 9. Surgeon's view through the frontotemporal orbitozygomatic (pterional) approach to the sellar region, illustrating the anatomical structures. ON, Optic nerve; SD, sellar diaphragm; ACLP, anterior clinoid process; ICA, internal carotid artery; rTL, right temporal lobe; I, olfactoric nerve; PS, pituitary stalk; rFL, right frontal lobe; III, oculomotor nerve; ACHOA, anterior choroidal artery; PCOMA, posterior communicating artery.

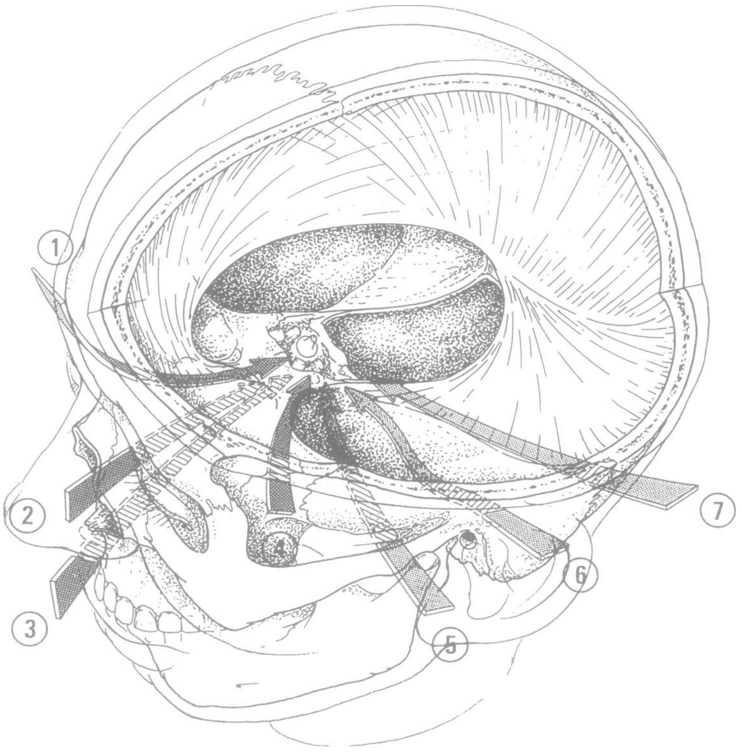

Figure 10. Schematic illustration of the different approaches to the sellar region. 1, transfrontal intradural approach; 2, transethmoidal-transsphenoidal approach; 3, transnasal-transsphenoidal approach; 4, frontotemporal orbitozygomatic (pterional) approach; 5, subtemporal intradural approach; 6, subtemporal-extradural approach; 7, temporooccipital approach.

three-dimensional mode, shows the relationship of pathological lesions to bony landmarks and osseous surface structures. Bone density and pneumatization of the skull base can also be exactly estimated with this technique. Digital subtraction and superselective angiography reveal small vessels beyond the resolution of three-dimensional CT and MRI angiography and enable preoperative embolization in interventional neuroradiology.[26,27]

For all that imaging techniques, preoperative planning, and elucidation of the patient's individual anatomy can do, further thorough intraoperative orientation is absolutely necessary.[18] For this purpose, the knowledge of distances, triangles, and morphological variations adds valuable information to the limited intraoperative view and the preoperative three-dimensional neuroimaging.

Thus, despite the modern techniques of neuroimaging and sophisticated neuronavigation, intraoperative orientation on landmarks in open or endoscopic surgery is essential.

REFERENCES

1. Perneczky A, Tschabitscher M, Resch KDM: Endoscopic Anatomy for Neurosurgery. New York: Thieme, 1993
2. Salvi G: Cavites prémandibulaires et des fossettes laterales de l'hypophyse chez les sauriens. Bibliogr Anat Paris X:131–137, 1902
3. Taptas JN: La loge du sinus caverneux; sa constitution et les rapports des eléments vasculaires et nerveux qui la traversent. Arch Ophthalmol Rev Gen Ophthalmol 16:404–412, 1956
4. Michailow SS: Makra- und mikroskopische Untersuchungen des Baues des Sinus cavernosus. Anat Anz 115:233–255, 1964
5. Bedford MA: The "cavernous" sinus. Br J Ophthalmol 50:41–46, 1966
6. Lang J: Eintritt und Verlauf der Hirnnerven (III, IV, VI) "im" Sinus cavernosus. Z Anat Entwickl Gesch 145:87–99, 1974
7. Lang J: Über die Pori durales der Nn III, IV und VI. Verh Anat Ges 69:785–791, 1975
8. Renn WH, Rhoton AL: Microsurgical Anatomy of the sellar region. J Neurosurg 43:288–298, 1975
9. Rhoton AL, Harris FS, Renn WH: Microsurgical anatomy of the sellar region and cavernous sinus. Clin Neurosurg 24:54–85, 1977
10. Lang J, Reiter U: Über den Verlauf des N. abducens vor der Austrittszone aus dem zentralnervösen Organ bis zum M. rectus lateralis. Neurochirurgia 28:1–5, 1985
11. Tsuha M, Aoki H, Okamura T: Roentgenological investigation of cavernous sinus structure with special reference to paracavernous cranial nerves. Neuroradiology 29:462–467, 1987
12. Taptas IN: La loge osteo durale parasellaire et les elements vasculaires et nerveux qui la traversent. Neurochirurgie 36:201–208, 1990
13. Ferner H: Die Beziehung der Leptomeninx und des Subarachnoidalraumes zur intrasellären Hypophyse beim Menschen. 2. Symp. d. Dt. Ges. f. Endokrinologie Goslar, 1954, pp 151–166
14. Lang J: In von Lanz T, Wachsmuth W (eds): Praktische Anatomie Band 1, 1. Teil, Teil B: Gehirn- und Augenschädel. Berlin: Springer, 1979
15. Dolenc VV: Anatomy and Surgery of the Cavernous Sinus. Wien: Springer, 1989
16. Umansky F, Valarezo A, Elidan: The superior wall of the cavernous sinus: A microanatomical study. J Neurosurg 81:914–920, 1994
17. Krmpotic-Nemanic J, Draf W, Helms J: Surgical anatomy of head and neck. New York: Springer, 1988

18. Samii M, Draf W: Surgery of the Skull Base. New York: Springer, 1989
19. Yasargil MG: Microsurgical Anatomy of the Basal Cisterns and Vessels of the Brain: Diagnostic Studies. General Operative Techniques and Pathological Considerations of the Intracranial Aneurysms. Stuttgart: Thieme-Stratton, Bd I, 1984
20. Sekhar LN, Burgess J, Akin O: Anatomical study of the cavernous sinus emphasizing operative approaches and related vascular and neural reconstruction. Neurosurgery 21:806–816, 1987
21. Bergland RM, Ray BS, Torack RM: Anatomical variations in the pituitary gland and adjacent structures in 225 human autopsy cases. J Neurosurg 28:93–99, 1968
22. Bonneville JF, Cattin F, Dietemann JL: Computed Tomography of the Pituitary Gland. Berlin: Springer, 1986
23. Krayenbühl H, Yasargil MG: Cerebral Angiography, 2nd ed. Stuttgart: Georg Thieme, 1982
24. Fahlbusch R, Buchfelder M: The transsphenoidal approach to invasive sellar and clival lesions. In Sekhar LN, Janecka IP (eds): Surgery of Cranial Base Tumors. New York: Raven Press, 1993
25. Teng MMH, Sartor K: Magnetic resonance imaging of the sellar and juxtasellar region. In Bonneville JF, Cattin F, Dietemann JL (eds): Computed Tomography of the Pituitary Gland. Berlin: Springer, 1986
26. Yasargil MG: Microneurosurgery, IV B, Microneurosurgery of CNS—Tumors. Stuttgart: Georg Thieme, 1996
27. Reul J, Spetzger U, Fricke C, Koner T, Bertalanffy H, Thron A: Endovaskuläre Behandlung zerebraler arterieller Aneurysmen mit selektiven ablösbaren Platinspiralen. Deutsche Med Wochenschr 120:669–675, 1995

We thank Mr. Peter Roth, Scientific Artist in the Neurosurgical Department, University Hospital of Zurich (CH), for his valuable encouragement in carrying out the illustrations.

REVIEWER'S COMMENTS

The authors present a carefully done anatomical study of the sellar region. They incorporate some novel anatomic concepts and provide a number of useful measurements. Although one is struck, as with prior studies of the anatomy of the sellar region, with the tremendous range of different measurements reflecting anomalies of the anatomy in this region, the fact that in an individual patient the various triangles are basically symmetrical with measurements that are similar from one side to the other is useful to know in planning surgery and in evaluating the distortion of normal anatomy produced by sellar pathology.

It is well known that in females, particularly those who have had a number of children, the diaphragmatic opening is frequently large. This is a result of intermittent swelling and contraction of the pituitary gland itself associated with pregnancy and is well demonstrated in the beautiful anatomical photographs. Any surgeon who has tried to dissect free the pituitary stalk knows that there are adhesions from the diaphragmatic dura to the stalk itself in a large number of patients, and these also are beautifully illustrated. This is an important point in dealing with some aspects of pituitary surgery, particularly those tumors that extend up the stalk and in those situations such as craniopharyngioma where the stalk needs to be carefully and atraumatically sectioned.

The anatomical details presented in this article will be beneficial to surgeons using any of the numerous approaches that have been illustrated and discussed by the authors. This article is a reminder as to how important knowledge of anatomy, and particularly the pathological changes in anatomy that occur in response to disease, may be in the planning of successful surgical therapy.

Edward R. Laws, Jr., M.D., F.A.C.S.
Charlottesville, Virginia